



Temperature-dependent viscometry of baobab pectin (*Adansonia digitata* L.)

Shadreck Muyambo ^{a,b,*}, Jack. A. Urombo^{c,d}

^aFosField Research & Development Co. (P/L), 25A Scott Road Hatfield, Harare, Zimbabwe

^bDepartment of Food Processing Technology, Harare Institute of Technology, Ganges Rd, Box BE 277, Belvedere, Harare, Zimbabwe

^cMathematical Sciences Department, Harare Institute of Technology, P.O. Box BE277 Belvedere, Harare, Zimbabwe

^dDepartment of Mathematics, Amity School of Applied Sciences(ASAS), Amity University Gurugram, Amity Education Valley Gurugram, Manesar, Panchgaon, Haryana 122412, India

Abstract

This study uses the Arrhenius-type equation and the Frenkel-Eyring equation to evaluate the viscosity-temperature dependency of the baobab pectin (BoP) solution at 278.16-353.16 K. The viscosity parameters (apparent viscosity, η_A and intrinsic viscosity, $[\eta]$) were analysed for polymeric systems of WEp (pectin extracted using water), AEp (pectin extracted using acid), and Cp (citrus pectin, a control). A Vibro-viscometer was used to measure η_A , while $[\eta]$ values were estimated from the Kuwara equation. The viscosity parameters decrease with an increase in temperature, though the effects were more pronounced in WEp than in AEp and Cp. Data from $[\eta]$ indicated that activation energy E_a was higher for AEp (12.24 kJ/mol) and lower for WEp (10.18 kJ/mol). In contrast, the η_A data had a higher E_a for WEp (21.38 kJ/mol) and a lower E_a for Cp (16.49 kJ/mol). The η_A data showed a non-linear viscosity-temperature relationship, and the Vogel-Fulcher-Tammann-Hesse equation was used instead to relate the temperature dependency of BoP. The flow patterns of all pectin solutions showed positive entropy (ΔS_v^+), positive enthalpy (ΔH_v^+), and negative Gibbs free energy (ΔG_v^-). This revealed that the flow was disordered, dependent on temperature, and spontaneous. Overall, the viscous flow of WEp was more sensitive and less dependent on temperature compared to AEp and Cp.

DOI:10.46481/asr.2024.3.1.146

Keywords: Baobab pectin, Viscosity-temperature dependency, Arrhenius parameters, Thermodynamic parameters

Article History :

Received: 01 August 2023

Received in revised form: 02 January 2024

Accepted for publication: 09 January 2024


Published: 08 February 2024

© 2024 The Author(s). Published by the Nigerian Society of Physical Sciences under the terms of the Creative Commons Attribution 4.0 International license. Further distribution of this work must maintain attribution to the author(s) and the published article's title, journal citation, and DOI.

1. Introduction

One of the fundamental features of polymeric molecules is their ability to portray certain configurations when temperature is increased or reduced. Such structural changes may have significance for the techno-functional properties of the polymeric material. *Adansonia digitata* L. (baobab) is one of the indigenous plants in Southern Africa known to have higher levels of pectic material in its leaves, buck, and fruits [1-3]. The extraction of pectin from the fruit, leaves, and buck has been done using alkaline, chelating agents, or acidic hydrolysis [1, 3, 4]. Pectic material from the baobab pulp found in the fruit has been extracted by hydrolysis in warm or hot water [2, 5, 6].

*Corresponding author: Tel.: +263-78-284-4569;

Email address: shadiemyambo@hotmail.com (Shadreck Muyambo )

Alba *et al.* [3], Damodaran *et al.* [4], Dimopoulou *et al.* [7], and Nwokocho and Williams [8] all mentioned the chemical properties of baobab pectin extracted using water and acid solvents. An experiment by Alba *et al.* [3] used NMR analysis and size exclusion chromatography coupled to a light scattering detector (SEC-MALS) to study the structure, molecular weight, and monosaccharide of BoP. They found that the leaves have linear and branched pectins with approximately 71 mol% uronic acids, 12 mol% rhamnose, and 9 mol% galactose. The fruit pulp, on the other hand, has about 69 mol% uronic acids and 13 mol% xylose (xylogalacturonans). Another unique thing about baobab pectin (BoP) is that it only has one β -Xylp (xylogalacturonans) residue, which replaced about 12 mol% of 1,4-linked α -GalpA (galacturonic acid) residues at the O-3 position [2-4]. Thus, the polysaccharide mainly constitutes linear xylogalacturonans [2, 3, 7, 8]. Studies showed that the average molecular weight of baobab pectin ranges from 30 kDa to values above 300 kDa [2-4]. Comparisons made at the point of extraction showed that pectic material from leaves had a high molecular weight (> 300 kDa), while that from fruit or pulp had a low molecular weight (< 200 kDa) [3]. The molecular weight of pectin from water extraction is lower (58 kDa), and its degree of esterification, dE lower ($dE < 20\%$). On the other hand, molecular weight of pectin from acid extraction is higher ($M_w > 300$ kDa) and its dE higher ($dE \approx 50\%$) [2, 3]. Patova *et al.* [2] and Alba *et al.* [3] extrapolated the intrinsic viscosity, $[\eta]$, of baobab pectin (from the water extraction method) using Huggins and Kraemer's equation at a concentration range of 0.52-1.63 g/dL and obtained a value of 0.038 L/g. Alba *et al.* [3] found that acid-extracted baobab pectin had an $[\eta]$ of 0.050-0.070 L/g, at concentrations of 0.01-25.0 g/dL, based on the Huggins and Kraemer equations.

The strength and quantity of interactions between polymer-polymer and polymer-solvent molecules typically govern the viscometric properties of polymers [9]. In general, an increase in the solution's viscosity provides a good explanation for how water interacts with pectin [10]. Thus, a drag of flow in pectin solution that is directly proportional to concentration is usually experienced [11]. Determination and analysis of intrinsic viscosity from pectins and related polysaccharides or biopolymers using several mathematical models were mentioned in the literature [12-17]. According to Masuelli [10], Pamies *et al.* [12], and Fellows [18], the flow properties of pectin can change from Newtonian to non-Newtonian. This depend on factors like the acid potential of the solvent, the presence of cations, changes in concentration, and temperature changes. Lopez *et al.* [19] indicated that the introduction of heat in a polymeric system may change the strength and the number of molecular interactions, which may alter the viscosity properties completely. There are long-standing theories on the effects of temperature on flow mechanics and the rate of reaction of molecules. A well-known phenomenon of temperature is its ability to reduce the viscosity (increase the flow rate) of solution and increase the rate of reaction as explained by Berthelot's exponential formula (Eq. 1) [20-22]. Thus,

$$K_1 = A \cdot B^{T_1}, \quad (1)$$

where K_1 is the reaction or flow velocity constant at the temperature T_1 ; A and B are constants of the equation.

Berthelot's formula (Eq. 1) presumes that K_1 increases in a geometrical progression when the temperature rises arithmetically. However, as illustrated by Belehradek [21], Berthelot's formula breaks down at higher temperatures. This constraint was rectified by the Van't Hoff empirical rule, which uses the ratio of the velocity constant (K_1 and K_2) of two temperatures (T_1 and T_2) differing by 10 degrees. This can be represented by Eq. (2) [23]:

$$\log \frac{K_1}{K_2} = A \cdot \left(\frac{T_1 - T_2}{T_1 \cdot T_2} \right) = A \cdot \left(\frac{10}{T_1 \cdot T_2} \right), \quad (2)$$

where K_1 and K_2 is the velocity constant at temperatures T_1 and T_2 respectively, and A is proportionality constant.

Perhaps the most popular theory for relating viscometry to temperature is the Arrhenius law or equation. Several studies [24-26] have used the Arrhenius equation to elucidate viscosity-temperature dependency in typical polymer solution systems. In the Arrhenius system, temperature dependence, T of reaction rate or viscous flow (K), is based on activation energy, E_a (temperature sensitivity), as shown in Eq. (3) [24, 27].

$$E_a = RT^2 \frac{d \ln K}{dT}, \quad (3)$$

Vyazovkin [24] showed that E_a from the Arrhenius equation can be related to Van't Hoff using the temperature coefficient of the rate change, Θ (a change in the rate constant per 10K change in temperature) using Eq. (4). Thus:

$$\ln \Theta \equiv \ln \frac{K_1}{K_2} = \frac{E_a}{R} \left(\frac{10}{T_1 \cdot T_2} \right). \quad (4)$$

Θ is the ratio of velocity constants for temperatures differing by 10 degrees, and its value is between 2 and 3 approximately [23, 28]. Using the Arrhenius equation, other models and interpretations have been developed. Ike [29] introduced the Arrhenius temperature (T) and Arrhenius activation temperature (T^*) for accessing transport behaviours in mustard oil and cotton seed oil at temperatures between 25 and 90°C. Ike [29] showed that E_a and pre-exponential factor are temperature-independent within 278.15-328.15K. Using graphical and linear least-fitting methods, the intercept can be used to find a third parameter, the Arrhenius temperature (T_A), along with the gradient (E_a/R) and intercept $\ln \eta_0$. T_A simplifies Eyring's viscosity-temperature dependence equation -an

Arrhenius-type equation that is suitable for a wider temperature range. Vogel-Fulcher-Tammann-Hesse (VFTH) type equation and the Frenkel-Eyring equation both add to the Arrhenius equation by incorporating non-Arrhenius ideas and thermodynamic concepts [24, 27].

There are other theories for the mechanistic interpretation of temperature-dependent fluid flow. The cooperatively rearranging region (CRR), which Adam and Gibbs proposed, mandates that structural units cooperate to reorganise themselves in order to achieve viscous flow [30, 31]. These theories imply that changes in molecular interactions brought about by bond breaking, switching, and twisting have an impact on the thermally activated viscous flow [32]. As a result, Cox and Merz [33] noted that an increase in molecules' kinetic energy, which allows them to pass the energy barrier (E_a), can define viscous flow. Alternately, transitions in the chemical interactions between sections of the pectin polymeric chain can explain viscous flow. As temperature increases, hydrophobic interactions between chain segments are promoted as compared to hydrogen bonding and van der Waals forces [34, 35]. So, as the temperature rises, temperature-initiated hydrophobicity makes interactions between polymers stronger than interactions between polymers and solvents. This causes the viscosity to decrease.

The temperature dependency of pectin solution and related polysaccharide, or biopolymers, is well established in the literature. Masuelli [10] and Masuelli [36] study the effects of temperature on the hydrodynamics of citrus pectin obtained from peels at a temperature range of 25-50°C. The studies conclusively indicated that the intrinsic viscosity of the pectin solutions decreases with an increase in temperature. The pectin behaves like a colloidal particle, with a rod-like conformation at low temperature that tends to compact with increasing temperature; that is, the hydrodynamic radius of the pectin molecules R_H decreased. It was also shown that the molecular weight of pectin was not affected by temperature (within the range of 25-50°C) but rather the hydrodynamic properties [10, 36]. Masuelli [10] further showed that there was an increase in E_a as concentration increased due to the high resistance to flow imposed by pectins. In another study, Kar and Arslan [37] also determined the effect of temperature on the viscosity of orange peel pectin solution at temperatures between 20 and 60°C. It was observed that intrinsic viscosity decreases as the thermal energy of molecules increases and the intermolecular distances increase due to thermal expansion. Using the Arrhenius equation, it was established that E_a depends on pectin concentration, and the effect of temperature was strong at higher concentration. Thus, both temperature and concentration have an effect on viscosity [37].

Zamani and Razavi [38] determined the effects of temperature on the flow of nettle seed gums (NSG) dispersed in distilled water at 10-70 °C. Intrinsic viscosity decreases with an increase in temperature. The shape factors of NSG at 10-40 °C was spherical, which changed to ellipsoidal as the temperature increased to 40-70 °C. Using the Arrhenius-type equation, Zamani and Razavi [38] found that NSG's E_a value was 0.488×10^7 J/mol and intrinsic viscosity ranged from 0.15-0.21 dL/g. Monkos [39] showed the viscosity-temperature dependency for human serum albumin (HSA) protein at temperatures ranging from 5-45 °C. Monkos [39] used Arrhenius and Mooney's equations to determine viscosity-temperature and viscosity-concentration dependence and establish that viscosity decreases with temperature and a relatively high solution's concentration increases the viscosity. Malviya [26] used the Arrhenius, Gibbs-Helmholtz, Frenkel-Eyring, and Eotvos equations to find surface tension, activation energy, Gibbs free energy, Reynolds number, and entropy of polymeric solution from tamarind seed at temperature of 10-80 °C. Apparent viscosity and surface tension decrease with an increase in temperature. Negative entropy and positive enthalpy were observed and suggest that bond breaking follows the attainment of the transition of viscous flow in tamarind seed gum. The lower values of Gibbs free energy obtained indicated that there were few intra- and intermolecular interactions.

Despite the fact that current literature has investigated the effects of heat on a variety of polysaccharides, gums, and biopolymers, no research has been conducted (to the best of our knowledge) on the temperature dependence of baobab pectin solution during flow. The study's objective was to use Arrhenius-type models and the Frenkel-Eyring equation to look at how the viscosity (both apparent and intrinsic viscosity) of BOP (extracted with water and acid hydrolysis) changes as the temperature varies. The research will be useful in developing heat-dependent processes that use baobab pectin for commercial purposes. As mentioned by Haj-Kacem *et al.* [27] and Muhidinov *et al.* [40], these processes can be extended to some of the following applications: hydraulic calculations for heat-dependent fluid transport; design processes such as retorting, microwaving, sterilisation, pasteurisation, freezing, thawing, and storage; and the development of products such as jams, jellies, beverages and pharmaceuticals.

2. Methodology

2.1. Extraction of pectins and preparation of analytes

Baobab pectin from the pulp was extracted using acid and water hydrolysis (Figure 1). The acid extraction method was obtained from Sundar Raj *et al.* [5], Sayah *et al.* [41], and Walding [42], with modifications. The baobab pulp was mixed with a citric acid solution (concentration = 20% or ≈ 1.04 M, pH=1.47), to make up 10% (w/v) of the baobab pulp solution with a pH of 1.56. The mixture was placed in a water bath at 80 ± 10 °C for 3 hours and stirred periodically. After cooling to approximately 55 °C, the solution was filtered using a double-folded mutton cloth or filter paper and then further cooled to room temperature. The water extraction method of pectin from baobab pulp was obtained from Patova *et al.* [2], Sundar Raj *et al.* [5], and Nour *et al.* [6] with modifications. Water extraction was done by suspending baobab pulp in distilled water using a ratio of 1:10 (10% w/v). The pH of the baobab pulp solution was 3.12. The mixture was heated in a water bath at 50 ± 5 °C for 1.5 hours, and stirring was done periodically. The slurry was filtered using a double-folded mutton cloth and cooled to room temperature. Pectin was precipitated from the filtrate

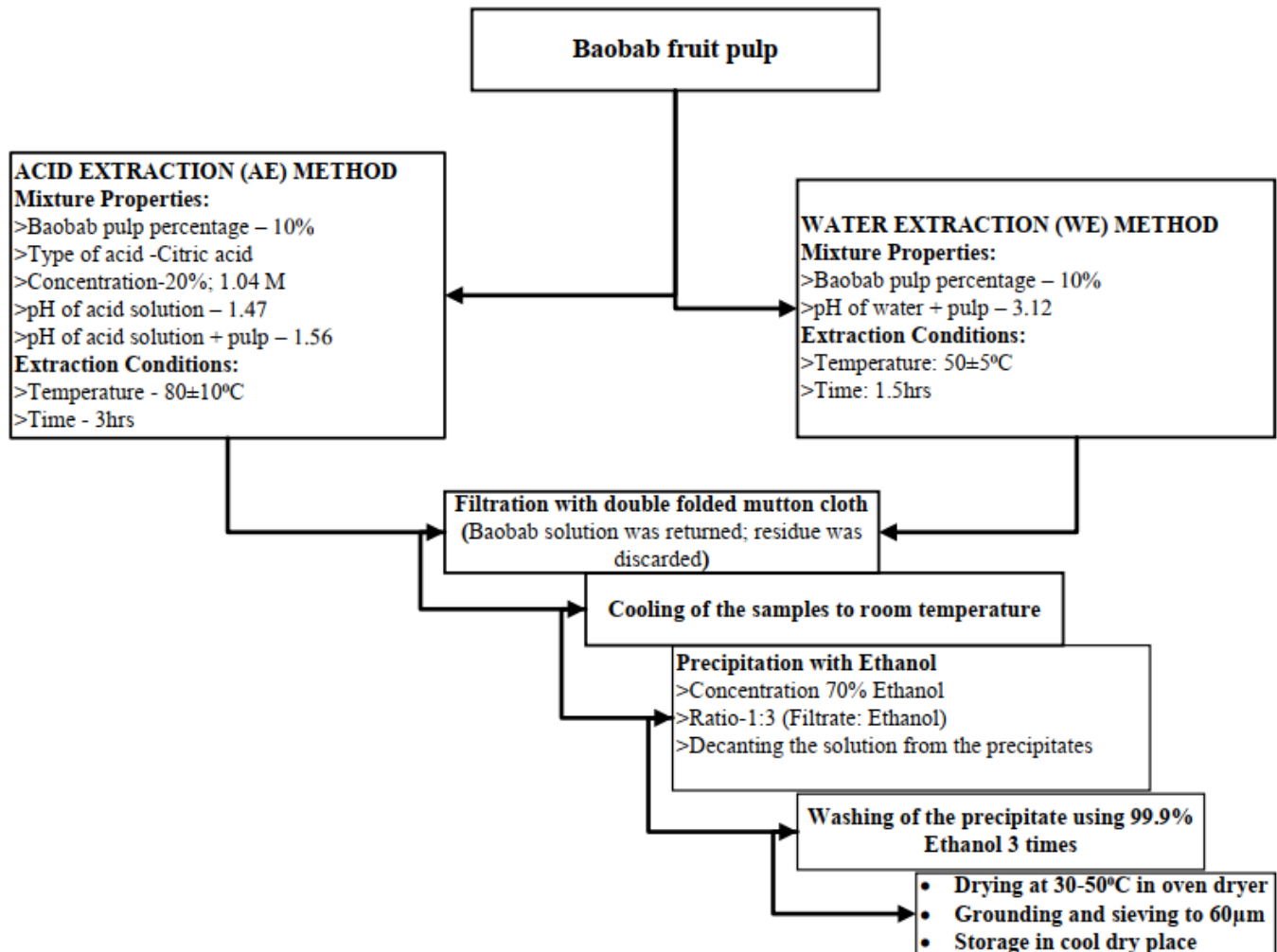


Figure 1: Flow chart for water (WE) and acid extraction (AE) methods.

with ethanol (70%) at a ratio of 1:3, and the liquid was decanted from the precipitate. The precipitate was washed with excess ethanol (99.9%) three times and then dried.

The extracted pectin precipitate was dried at 30-50 °C for approximately 9-10 hours using a forced draft oven (UL 40, Memmert, USA). After the drying process, the pectin extract was cooled in a desiccator, grounded, and sieved using a 60µm sieve aperture. The yellowish baobab pectin (BoP) powder was collected and stored in a dry, cool place. A commercial citrus high-methoxyl pectin, Cp (Grindsted pectin AMD 780, DM = 70%, Danisco, USA), and distilled water were used as reference samples. Analytes of pectin samples with a concentration of 2.0 g/dL were prepared by mixing respective amounts of pectin extract (2.0g) in distilled water (100ml). The mixture was mixed vigorously and allowed to stand for 24 hours at room temperature to allow complete hydration. The solutions were made for each sample of commercial pectin (Cp), water extraction baobab pectin (WEp), and acid extraction baobab pectin (AEp).

2.2. Viscosity and temperature measurement

A Vibro-viscometer (SV-10, A & D Company Limited) was used to measure pectin solutions' apparent viscosity (η_A), and Ostwald glass capillary apparatus to get intrinsic viscosity ($[\eta]$). The Vibro-viscometer was calibrated using distilled water within a temperature range of 5.0-60.0 °C. The effects of temperature on the flow properties of baobab pectin were investigated at approximately 5.0, 25.0, 50.0, and 80.0 °C. Temperature control was maintained using a water bath, which was set at the respective temperatures mentioned above. The sample was initially heated to the recommended temperature before being placed in a Vibro-viscometer or Ostwald apparatus. The flow time in the Ostwald viscometer was measured with the apparatus submerged in the water bath. However, for the Vibro-viscometer we measured the temperature before and after the measurement and used the average of the two temperature values. The average temperature, $T_{a,b}$ was calculated as follows (Eq. 5):

$$T_{a,b} = \left(\frac{T_a + T_b}{2} \right), \quad (5)$$

where T_a and T_b are the initial temperature (before measurement) and final temperature (after measurement), respectively.

2.2.1. Intrinsic viscosity calculation

An Ostwald capillary viscometer was used to measure the relative time taken by pectin solutions to flow through the capillary tube, as explained by Muyambo *et al.* [15] and Masuelli [36]. The tests were done in triplicate. The relative time (s) was used to calculate the viscosity ratios: relative viscosity η_r and specific viscosity (increment of relative viscosity) η_{sp} , as shown in Eq. (6) and Eq. (7) [13, 15, 43, 44].

$$\text{Relative viscosity, } \eta_r = t_s/t_0, \quad (6)$$

$$\text{Specific viscosity, } \eta_{sp} = (t_s - t_0)/t_0 = \eta_r - 1, \quad (7)$$

where t_s and t_0 are the time taken by BoP solutions and distilled water, respectively, to flow through the Ostwald capillary viscometer.

The viscosity ratios were used in the estimation of the intrinsic viscosity $[\eta]$ of the baobab pectin (BoP) solution. As mentioned by Pamies *et al.* [12], Muyambo [43], Abel-Azim *et al.* [45], Mahanta and Pattnayak [46], the prediction of $[\eta]$ used the Kuwahara equation (Eq. 8) is based on a single-point determination. Muyambo *et al.* [15], Masuelli [44], and Mahanta and Pattnayak [46] states that the single-point methods of evaluating (SPME) viscosity are better than the graphical extrapolation of experimental data (GEED) method because they save time and solvents while giving accurate results that are similar to the GEED method. The Kuwahara equation (Eq. 8) was used in this study since it is considered more accurate [43, 46].

$$\text{Kuwara Equation, } [\eta] = \frac{1}{4 \cdot c} (\eta_{sp} + 3 \ln \eta_r), \quad (8)$$

where c is the concentration in g/dL of the BoP solution.

2.2.2. The Arrhenius equation and Arrhenius parameters

The flow properties were related to temperature using the Arrhenius equations, Eq. (9), Eq. (10), and Eq. (11). Vyazovkin [24], Haj-Kacem *et al.* [27], Muhidinov *et al.* [40], and Ouerfelli *et al.* [47] all mentioned the Arrhenius equation for relating viscosity to temperature.

$$\eta = \eta_0 \exp[E_a/RT_K], \quad (9)$$

thus,

$$\ln \eta = \ln \eta_0 + \frac{E_a}{R} \cdot (1/T_K). \quad (10)$$

Messaadi *et al.* [25], Haj-Kacem *et al.* [27], and Ike [29] indicated that T^* equals the parameter E_a/R , termed the Arrhenius activation temperature or Boltzmann factor (Eq. 11). Thus, it follows that:

$$\ln \eta = \ln \eta_0 + T^* \cdot (1/T_K), \quad (11)$$

where η_0 is the pre-exponential factor (L/g) based on $[\eta]$ or η_A , E_a is the activation energy (J/mol), T_K is the absolute temperature in Kelvins (K), R is the universal gas constant (8.3144721 J/mol) and T^* is the Arrhenius activation temperature (K). The Arrhenius temperature, T_A (K), was calculated by using Eq. (12) as indicated by Messaadi *et al.* [25] and Haj-Kacem *et al.* [27]:

$$T_A = \frac{-E_a}{R \cdot \ln \eta_0}. \quad (12)$$

2.2.3. Pseudo-Arrhenius equations for non-linear flows

The agreement of the viscosity-temperature data to the Arrhenius equation was evaluated using the correlation coefficient (R^2) and root mean square errors (RMSE). The data, which had relatively low R^2 (< 90) values and high RMSE, was further fitted into non-linear mathematical models derived from Arrhenius equations [25, 27, 48], (Eq. 13 - 16):

$$\eta = \eta_0 \cdot \exp[(B + D/T_K) \cdot 1/T_K], \quad (13)$$

$$\eta = \eta_0 \cdot \exp[B \cdot 1/(T_K - C)], \quad (14)$$

$$\eta = \eta_0 \cdot \exp[a \cdot \log T_K + D/T_K], \quad (15)$$

$$\eta = \eta_0 \cdot \exp[B/T_K + b \cdot T_K], \quad (16)$$

where η_0 is the intercept and a , B , b , C , and D are proportionality constants.

Table 1: Intrinsic viscosity distribution at different temperatures using Kuwara equation.

WEp			AEp			Cp		
$T_\theta(^{\circ}C)$	T_K (K)	$[\eta]$ (L/g)	$T_\theta(^{\circ}C)$	T_K (K)	$[\eta]$ (L/g)	$T_\theta(^{\circ}C)$	T_K (K)	$[\eta]$ (L/g)
5.53	278.69	0.0132±0.009aA	5.10	278.26	0.0798±0.048aB	4.93	278.09	0.0912±0.078aC
24.97	298.12	0.0092±0.006bA	25.10	298.26	0.0427±0.001bB	24.97	298.13	0.0578±0.002bC
50.10	323.26	0.0081±0.007bA	50.27	323.43	0.0341±0.009cB	50.17	323.33	0.0432±0.003cC
79.00	352.16	0.0050±0.003cA	79.33	352.49	0.0247±0.003dB	79.00	352.16	0.0336±0.002dC

Values are expressed as mean±SD of three replicates.

Results with the same letters 'a - d' in a column are similar, $P > 0.05$.

Results with the same letters 'A - C' in a column are similar, $P > 0.05$.

2.2.4. The Frenkel-Eyring equation and Thermodynamic parameters

The Frenkel-Eyring equation (Eq. 17) from Vyazovkin [24], Malviya *et al.* [26], Acevedo and Kartz [49], and Sillick and Gregson [50] served as a basis for estimating the thermodynamic parameters of pectin solutions.

$$\ln\left(\frac{\eta}{T_K}\right) = \left(\ln \eta_0 - \frac{\Delta S_v}{R}\right) + \frac{\Delta H_v}{R} \cdot \left(\frac{1}{T_K}\right), \quad (17)$$

where η_0 is the pre-exponential factor, T_K is the absolute temperature, ΔS_v (J/K) is the change in entropy, R is the universal gas constant, and ΔH_v (J/mol) is the enthalpy of change in viscous flow.

A plot of $\ln(\eta/T_K)$ vs. $1/T_K$ is estimated to be linear with a slope equal to $(\Delta H_v/R)$, and an intercept equal to $(\ln \eta_0 - \Delta S_v/R)$ according to Malviya *et al.* [26] and Acevedo and Kartz [49]. Vyazovkin [24] and Acevedo and Kartz [49] showed that using the pre-exponential factor (η_0) obtained from the Arrhenius equation, the Gibbs free energy can be calculated at any absolute temperature, T_K , using the Gibbs-Helmholtz equation (Eq. 18):

$$\Delta G_v = \Delta H_v - T_K \cdot \Delta S_v, \quad (18)$$

where ΔG_v (J) is the Gibbs free energy.

2.3. Statistical analysis

The values were expressed as mean±SD for the 3 replicates conducted during the experiments. Using Fischer's Least Squares Differences (LSD) test at $P = 0.05$, significant differences between each pectic solution (WEp, AEp, and Cp) at different temperatures were determined. Statistical software packages used for data analysis and visualisation were SPSS (IMB SPSS Statistics, v26.0), MATLAB (MathWorks, R2018a), and Excel (Microsoft 2019).

3. Results and Discussion

3.1. Effects of temperature on intrinsic viscosity and apparent viscosity

The results for intrinsic viscosity $[\eta]$, at 278.69-352.16K, calculated using the Kuwahara equation (Eq. 8) are shown in Table 1. Table 2 shows the apparent viscosity (η_A) values as temperature increases from 278.18-353.16K. In addition, the apparent viscosity of distilled water was also determined as a control (Table 2). There was a big difference in the intrinsic viscosity values as the temperature rose and as the type of pectin changed (Table 1), with a significance level of $P < 0.05$ using LSD post-hoc.

The values for η_A are shown in Table 2. Using total means, it was observed that η_A from 298.16-323.16K was statistically the same, $P > 0.05$, (Table 2) but different from results observed at 278.16K. Table 2 shows that the total means for AEp and Cp were statistically the same using LSD post-hoc analysis in the same row. In general, higher values for intrinsic viscosity and apparent viscosity values were observed at low temperatures and decreased as temperatures increased (Figures 2 and 3). In both the cases of $[\eta]$ and η_A the graphs (Figure 2 and Figure 3, respectively) showed a step decrease in viscosity from 278K to 300K, which fattens out as temperature increases to 353K. Convincingly, the results for pectin samples showed that the $[\eta]$ and η_A of WEp were lower at any given temperature interval, while Cp showed the highest values (Figures 2 and 3).

3.2. Analysis of the temperature-dependency of pectins using the Arrhenius parameters

The Arrhenius parameters for the dependency of intrinsic and apparent viscosity on temperature are shown in Table 3. The Arrhenius plots for $[\eta]$ and η_A are shown in Figure 4 and Figure 5, respectively. In general, $[\eta]$ data points were close to the line of best fit (Figure 4) compared to η_A data (Figure 5). This was in agreement with correlation coefficient (R^2) values in Table 3 which are higher in $[\eta]$ than η_A . Such dispersions may suggest that $[\eta]$ data is more linear, while η_A is not perfectly linear.

Table 2: Apparent viscosity of baobab pectin (BoP) samples at different temperatures.

		Apparent viscosity, $\eta_A \times 10^{-3}$ (Pa.s)				Total mean
T_θ ($^\circ\text{C}$)	T_K (K)	WEp	AEp	Cp	dW	Mean \pm SD
5.0	278.16	8.70	30.10	39.30	3.17	14.1 \pm 10.7a
25.0	298.16	2.03	10.00	10.20	0.67	4.05 \pm 3.99b
50.0	323.16	1.38	6.87	7.40	0.50	2.75 \pm 2.75b
80.0	353.16	1.09	5.31	7.93	0.47	2.15 \pm 2.11b
Mean \pm SD		3.30 \pm 3.62A	13.1 \pm 11.52B	16.2 \pm 15.44B	1.21 \pm 1.31A	

Total mean \pm SD with the same letters 'a - b' in a column are similar, $P > 0.05$.

Total means \pm SD with the same letters 'A - B' in a column are similar, $P > 0.05$.

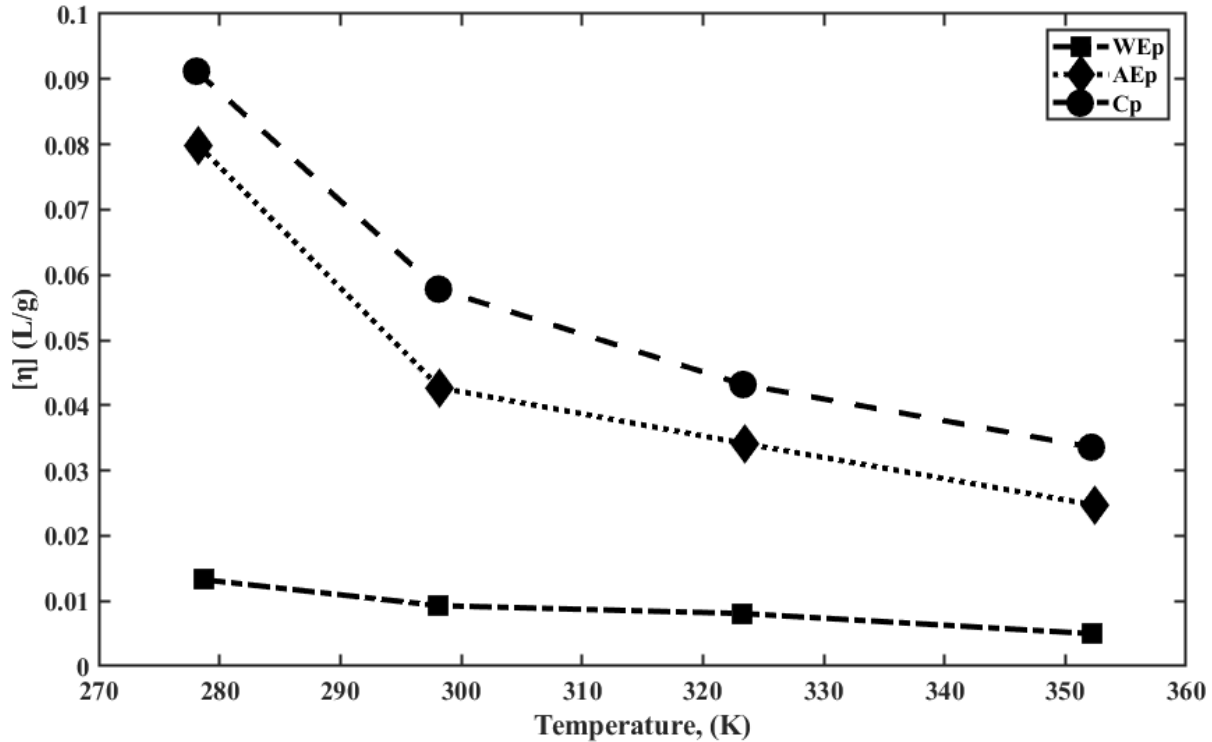


Figure 2: Change of intrinsic viscosity with temperature.

Table 3: Shows the Arrhenius parameters for both $[\eta]$ and η_A data.

Intrinsic viscosity, $[\eta]$ data							
	$\ln \eta_0$	η_0	$E_a/R = T^*$ (K)	E_a (kJ/mol)	T_A (K)	R^2	RMSE
WEp	-8.72	0.000163	1224	10.176	140	0.958	0.1015
AEp	-7.933	0.000358	1473	12.246	186	0.945	0.1427
Cp	-7.125	0.000805	1298	10.792	182	0.976	0.0816
Apparent viscosity, η_A data							
dW	-14.59	4.61×10^{-7}	2335	19.413	160	0.731	05711
WEp	-14.37	5.74×10^{-7}	2572	21.384	179	0.826	04757
AEp	-11.57	9.44×10^{-6}	2172	18.058	188	0.875	0.3312
Cp	-10.77	2.09×10^{-5}	1983	16.487	184	0.697	0.5273

* Units for pre-exponential factor for intrinsic viscosity data are (L/g) and (Pa · s) for apparent viscosity data

The pre-exponential or entropic factor (η_0) values were observed to range around 10^{-4} L/g for intrinsic viscosity values and from 10^{-5} to 10^{-7} Pa.s for apparent viscosity (Table 3). The pre-exponential factor value increases with the order: $WEp < AEp < Cp$ for both the $[\eta]$ and η_A data. According Messaadi *et al.* [25], the pre-exponential factor is associated with motion in a polymer system

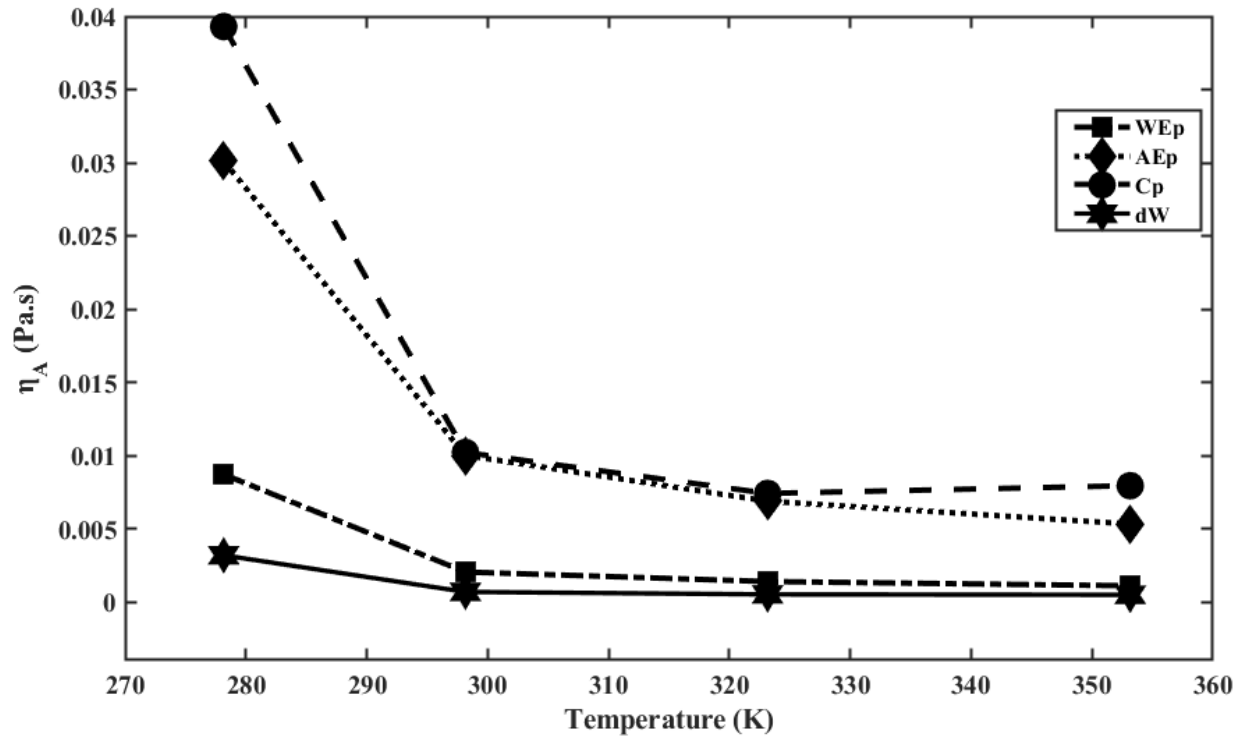


Figure 3: Distribution of apparent viscosity with temperature.

independent of temperature. The η_0 is the viscosity at infinite temperature or at zero activation energy (barrier-less) [25, 29, 50]. The entropic factor is satisfied when the Boltzmann factor $[\exp(E_a/RT_K)] = 1$. This means that $E_a/RT_K = 0$, which follows that either T_K should be infinite or E_a should be zero, and hence no barriers for polymeric flow [50]. In other words, according to Messaadi *et al.* [25] and Ike [29], η_0 is independent of temperature and activation energy, and as a result, when $E_a \rightarrow 0$, $\ln \eta_0 \neq 0$.

A lot of authors have reported that the pre-exponential or entropic factor is the number of molecules that have enough kinetic energy to start a reaction or move at zero activation energy [25, 51, 52]. Based on these relationships, we can generalise that the entropic factor (shown in the viscosity-temperature Arrhenius equation) indicates the fraction of molecules that need to attain enough kinetic energy for a viscous flow to be experienced. This means the higher the η_0 is, the greater the fraction of molecules that should have enough kinetic energy for temperature-independent motion to commence at zero activation energy or infinite temperature. So, in WEp, fewer molecules are needed to gain enough kinetic energy for the solution to flow at zero E_a than in AEp and Cp, where a larger number of molecules may be needed, as shown in Table 3. Meaning that the flow of WEp is less dependent of temperature as compared to AEp and Cp.

The Arrhenius activation temperature is also shown in Table 3 as $T^* = E_a/R$; this is essentially the gradient from the Arrhenius plot (Figures 4 and 5). T^* indicates the amount of heat required for molecules to attain kinetic energy that exceeds the activation energy [25]. The significance of the T^* is the approximation of the E_a and further its interpretation of the Arrhenius temperature (T_A, K). The Arrhenius temperature, T_A is the temperature associated with the pre-exponential factor $\ln \eta_0$. By recalling Eq. (12), it can be generalised that the product of $T_A \ln \eta_0 = E_a/R = T^*$. The negative sign was ignored since the product $T_A \ln \eta_0$ is usually negative as η_0 is always small, hence they will cancel out. Thus, in fact, $T_A < T^*$ (Table 3), and hence, it can be used as a reference temperature in the Eyring type equation for solving viscosity-temperature dependency, [25, 53].

It was observed that the greater the T_A value required by a polymeric system, the greater its activation energy, E_a (Eq. 12). This agrees with the results shown in Table 3. The higher the T_A value of the AEp polymeric system, the higher its corresponding E_a value. The lower the T_A , as in WEp or Cp, the lesser the E_a values. Messaadi *et al.* [25] and Ike [29] showed that T_A is exponentially related to E_a using the following expression (Eq. 19):

$$T_A = [\exp(-\alpha E_a) - 1 / -\beta], \quad (19)$$

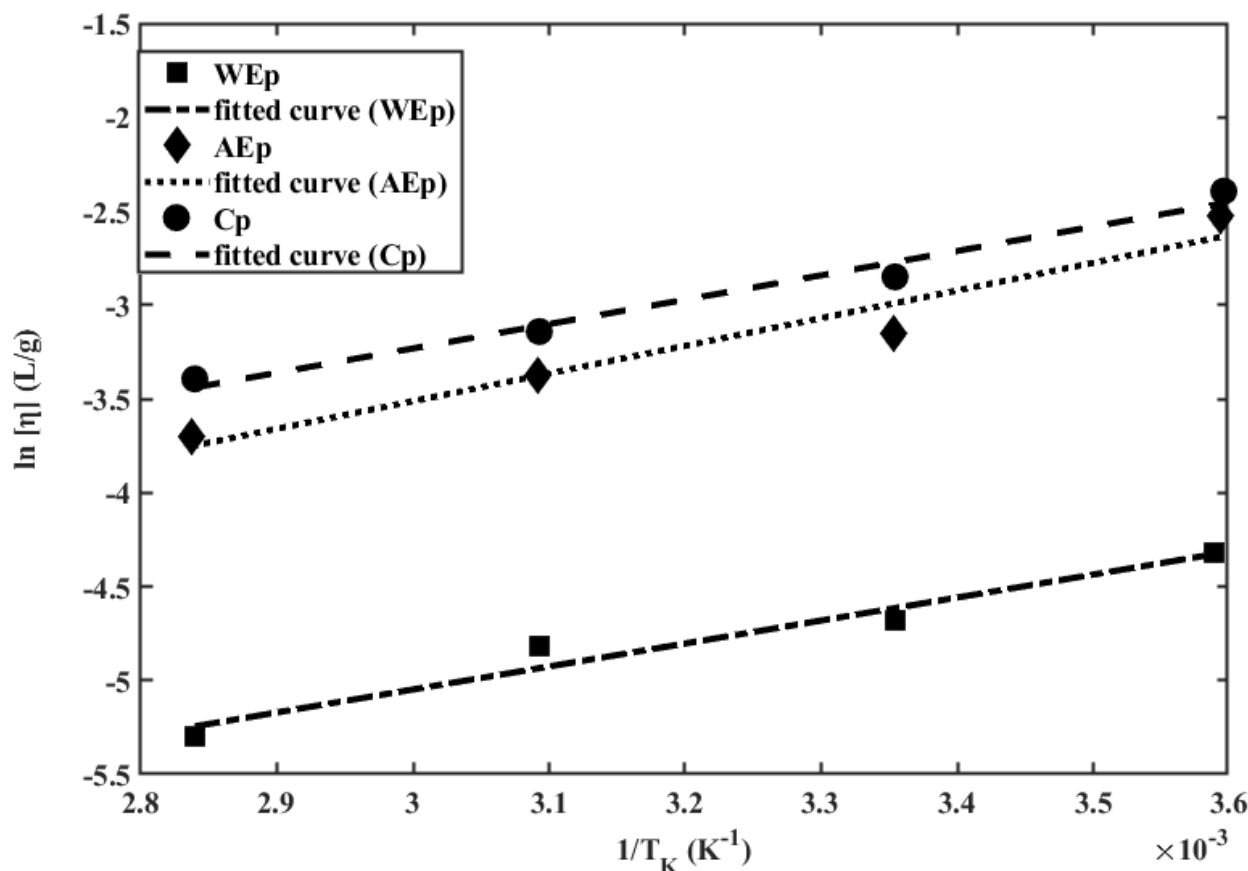


Figure 4: Arrhenius plot for intrinsic viscosity data of WEp, AEp, and Cp pectins.

where α, β are proportionality constants.

The exponential expression, Eq. (19), showed that when $T_A \rightarrow 0$; $\ln \eta_0 \neq 0$, but however, as $E_a \rightarrow \infty$; $T_A \rightarrow 0$. Thus, there is a limit value that T_A is approaching (T_{lim}) before the temperature reaches the Arrhenius activation temperature T^* [25, 29]. This means the polymer's kinetic energy increased in stages, like from T_A to T_{lim} until T^* . At the Arrhenius activation temperature (T^*) the kinetic energy gained will now be equal or above the energy barrier, E_a , and hence, viscous flow begin.

The activation energy E_a has been mentioned previously, as has its geometrical relationship with other Arrhenius parameters. The values of E_a found from $[\eta]$ data were 10.17 kJ/mol for WEp, 12.25 kJ/mol for AEp, and 10.79 kJ/mol for Cp. The values found from η_A data were 21.4 kJ/mol for WEp, 18.1 kJ/mol for AEp and 16.5 kJ/mol for Cp (Table 3). Based on $[\eta]$, the E_a values decrease in the order: $AEp > Cp > WEp$. This means more heat is needed to initiate flow in the AEp solution than in Cp and WEp. The range of E_a values noticed in this study is comparable to those of other polysaccharides mentioned by Masuelli [10] on citrus peel pectin (6.01 kJ/mol); Kar and Arslan [37] on orange peel pectins (19.5-27.2 kJ/mol); Malviya *et al.* [26] on tamarind seed gums (20.5 ± 1.06 kJ/mol); de Paula *et al.* [54] for Albizia lebbeck gums (15.9-17.2 kJ/mol) and de Paula and Rodrigues [55] for *A. occidentale* gum (16.2 kJ/mol). Rao [22], and Mezger [56] explained that E_a is interrelated to the energy barrier needed by molecules to transcend from one local flow state to the next. This can be thought of as the energy required by molecules to move between adjacent layers in the laminar flow of fluids. Vyazovkin [24] and Berk [57] state that E_a is related to how sensitive a defined polymeric system is to temperature. The lower the E_a value, the higher the sensitivity, and this means that the solution is more likely to have viscous flow. On the other hand, Shaikh *et al.* [58] explained that the higher the activation energy, the greater the pectin solution's temperature dependence for viscous flow.

Table 3 also shows that the trend for E_a values obtained from $[\eta]$ gets violated when viewing the apparent viscosity, η_A . For instance, E_a decreases in the following order: $WEp > AEp > Cp$ for η_A data. Such a difference was attributed to the method used to obtain the η_A and $[\eta]$. The results for η_A in Table 3 are in contrast to the idea that solutions with high viscosity have high E_a since in Eq. (10) $\ln \eta \propto E_a$. Masuelli [10], Malviya *et al.* [26], and Kar and Arslan [37] all supported this. Thus, E_a was expected to be

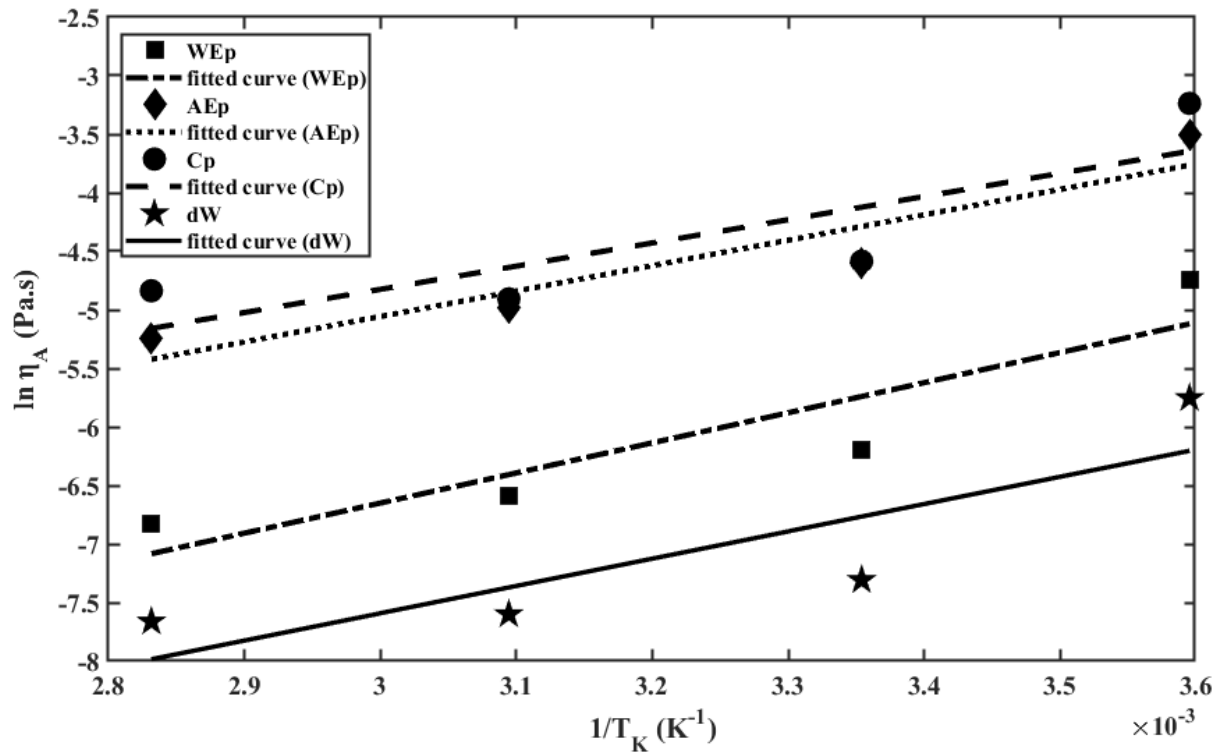


Figure 5: Scatter plot of apparent viscosity and temperature for WEp, AEp, and Cp.

higher for Cp and AEp and at its lowest for WEp and dW. However, this behaviour is satisfied by purely linear relationships (Figure 4, $[\eta]$ data), suggesting a non-linearity behaviour between $\ln \eta_A$ and $(1/T_K)$ (Figure 5). The fact that the R^2 values are low and the RMSE is higher (Table 3) than it was for $[\eta]$ data is also proof of non-linearity. Messaadi *et al.* [25] and Ike [29] indicated that for the Arrhenius equation to be linear, E_a and $\ln \eta_0$ should be independent of temperature, and this is possible for temperature ranges between 278.16-328.16K. In this study, temperatures higher than this were used, i.e., 353.16K, affecting the linear progression of the changes of $\ln \eta_A$ with $(1/T_K)$. In these situations, E_a will depend on temperature, and the basic Arrhenius equation will not be good enough to approximate the E_a values. This is why we need non-Arrhenius-type equations (Table 4, Eq. 13-16).

Table 4 shows that the best fit model was Eq. (14), which has higher R^2 values (0.9996) and relatively low root mean squared errors (RMSE) as compared to other models. Figure 6 shows the graph obtained after fitting Eq.14. Comparison of Figure 5 (linear fit) and Figure 6 (non-linear fit) showed that the η_A data points were close to the line of best fit in Figure 6. Thus, the dispersion of η_A data followed an exponential curve rather than a straight line in Arrhenius plots.

The model (Eq. 14) was recognised to be similar to the Vogel-Fulcher-Tammann-Hesse (VFTH) type equation (Eq. 20), as mentioned by Haj-Kacem *et al.* [27], Muhidinov *et al.* [40], Ouerfelli *et al.* [47], and Tammann and Hesse [48].

$$\ln \eta = \ln \eta_0 + \frac{E_a}{R} \left(\frac{1}{T_K - T_0} \right), \tag{20}$$

A comparison of Eq. (14) and Eq. (20) can easily show that T_0 is analogous to constant C and B to the gradient (E_a/R). Liew and Ramesh [59] indicated that the VFTH model is valid for temperatures ranging from ambient to 328.18K, which are basically the temperature regimes used in this study; however, it is still lower than 353.16K. Thus, in other terms, the VFTH equation is a special case of the Arrhenius equation (with $T_0 = 0$) [60]. Table 5 shows the VFTH parameters obtained using Eq. (20).

The distribution of the pre-exponential factor, shown in Table 5, revealed that the values decreased in the order: $Cp > AEp > WEp > dW$. This was similar to the trend obtained from the Arrhenius equation (Table 3) for intrinsic viscosity, and the $\ln \eta_A$ was proportional to E_a , as expected earlier. It was found that the activation energy dropped by about 100 times compared to the values found using the Arrhenius equation (Eq. 10 and Table 3). Also, the pre-exponential factor η_0 went up (range $10^{-4} - 10^{-3} Pa \cdot s$). Sogabe *et al.* [60] and Angell [61] mention η_0 values (obtained using the VFTH equation) in the order of $10^{-5} Pa \cdot s$ for many kinds

Table 4: Non-linear Arrhenius based equation for relating apparent viscosity and temperature.

		Constants							
		$\ln \eta_0$ (L/g)	B	D	C	a	b	R^2	RMSE
Eq. 13	$\eta = \eta_0 \cdot \exp[(B + D/T_K) \cdot 1/T_K]$								
	dW	46.15	-3.6×10^4	5.9×10^6				0.9719	0.2605
	WEp	35.77	-2.9×10^4	4.9×10^6				0.9792	0.2328
	AEp	23.51	-2.0×10^4	3.4×10^6				0.9861	0.1564
	Cp	46.91	-3.4×10^4	5.6×10^6				0.9841	0.1707
Eq. 14	$\eta = \eta_0 \cdot \exp[B \cdot 1/(T_K - C)]$								
	dW	-7.857	14.46		271.4			0.9996	0.0304
	WEp	-7.184	33.59		264.4			0.9996	0.0329
	AEp	-5.679	43.51		258.2			0.9992	0.0365
	Cp	-5.032	10.92		272.1			0.9934	0.1103
Eq. 15	$\eta = \eta_0 \cdot \exp[a \cdot \log T_K + D/T_K]$								
	dW	-824.2		4.0×10^4		120		0.9657	0.2886
	WEp	-682.2		3.4×10^4		99.0		0.9750	0.2553
	AEp	-478.9		2.4×10^4		69.3		0.9837	0.1721
	Cp	-782.7		3.7×10^4		114		0.9789	0.1966
Eq. 16	$\eta = \eta_0 \cdot \exp[B/T_K + b \cdot T_K]$								
	dW	-134.0	2.1×10^4				0.19	0.9625	0.3014
	WEp	-112.8	1.8×10^4				0.15	0.9775	0.2662
	AEp	-80.48	1.3×10^4				0.11	0.9816	0.1798
	Cp	-124.8	2.0×10^4				0.18	0.9761	0.1813

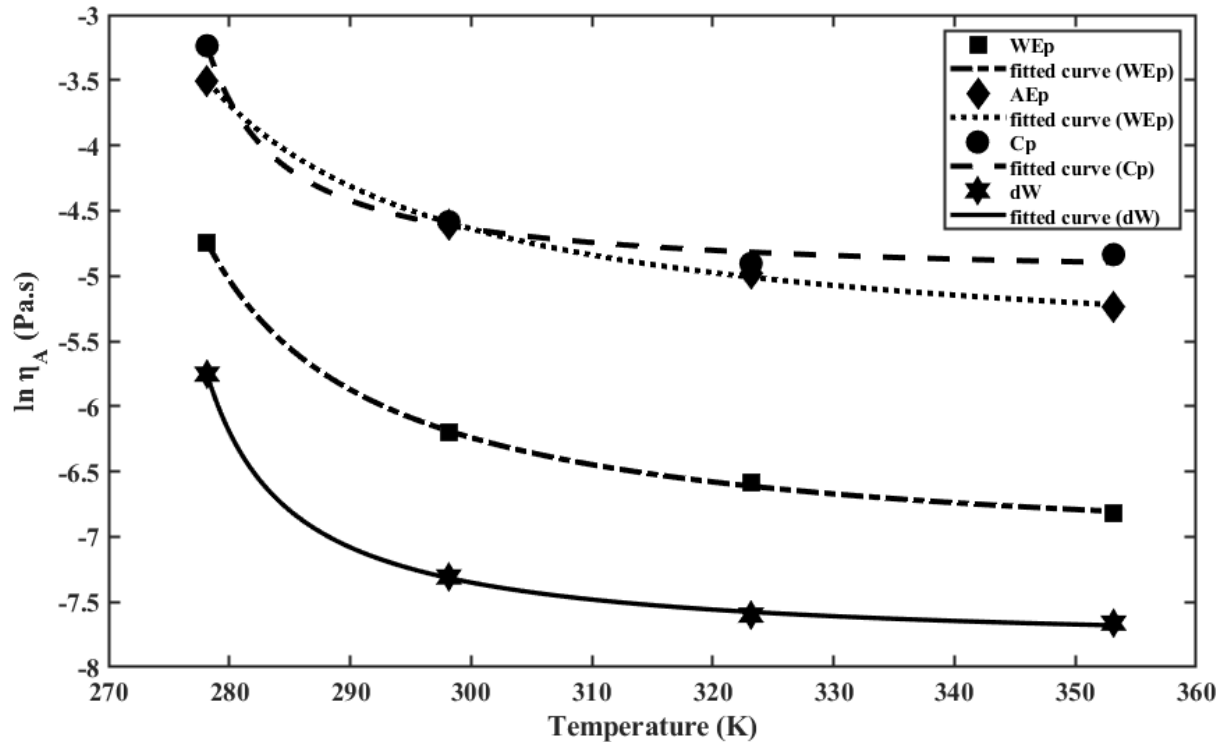


Figure 6: Non-Linear Arrhenius plot (Vogel-Fulcher-Tammann-Hesse (VFTH)-type equation).

of liquids and carbohydrate-water systems. This η_0 value was lower than those obtained in this study using the VFTH model but related to values from the Arrhenius equation. However, the value of η_0 for the VFTH model obtained in this study is the same range as that from intrinsic viscosity data.

Table 5: Parameters for non-linear Arrhenius equation (Vogel-Fulcher-Tammann-Hesse (VFTH) type equation, Eq. 20).

Pectin	η_0 (L/g)	$T^* = \frac{E_a}{R}$ (K)	E_a (kJ/mol)	T_0 (K)	R^2	RMSE
dW	0.000387	14.46	0.120	271.4	0.9996	0.0304
WEp	0.000759	33.59	0.279	264.4	0.9996	0.0329
AEp	0.003417	43.51	0.362	258.2	0.9992	0.0365
Cp	0.006526	10.92	0.091	272.1	0.9934	0.1103

It was found that the Vogel scaling temperature, also known as the vitreous transition temperature, T_0 [34, 61], caused the differences between the Arrhenius and VFTH models. T_0 values were observed to range from 258.2-272.1K (Table 5). The T_0 decreases with increasing apparent viscosity. Thus, T_0 decreases in the order: $dW > WEp > AEp$. However, an anomaly was seen in the Cp data, though it has the highest η_A values. The T_0 was surprisingly higher (272.1K) almost the same as that of distilled water, dW (271.4K), Table 5. We anticipated the T_0 value for Cp to be the lowest based on the trend that dW, WEp, and AEp displayed. Such a deviation could have arisen from the inability of the VFTH to fit the data well. A decrease in the R^2 was observed in the Cp data (Table 4 and 5). Thus, the temperature dependence (i.e., the degree at which viscosity changes with an increase in temperature) of Cp's apparent viscosity was beyond the boundaries of the VFTH equation.

The implication of T_0 is its representation and linear relationship with the glass transition temperature, T_g . Sillick and Gregson [50], and Liew and Ramesh [59] stated that T_0 is approximately 50K below the T_g (kinetic glass transition temperature) and above 0.0K. When $T_K \rightarrow T_0$ (considering Eq. 20), the viscosity will approach infinity. However, this feature of the VFTH equation was regarded as causing a systematic error at low temperatures [50]. According to Franks [62], Roos and Karol [63], and Sillick and Gregson [50], T_0 shifts upwards by an amount that has strong dependence on molecular weight M_w .

Angell *et al.* [64] explanation of T_0 was based on the concept of fragility. Glass-forming liquids (like pectin solution) that obey the Arrhenius equation are classified as strong-fragile and are termed strong systems [60, 62, 64, 65]. In a strong-fragile system, this means that when viscosity ($\ln \eta$) is plotted against ($1/T_K$), a straight line is seen, as shown in Figures 2 and 4. Opposite to the strong-fragile class are the fragile systems, which are characterised by a curvature in the viscosity-temperature dependency plot due to the dependency of E_a on temperature, as explained earlier (Figure 6). In such cases, the relationship will not obey the Arrhenius behaviour but rather obey the VFTH type equation, as later observed in the apparent viscosity data [32]. Thus, keeping the fragility concept in mind, T_0 can be thought to indicate the dynamical divergence in the temperature dependency of a viscous system [64, 65]. Sogabe *et al.* [60] showed that polysaccharide solutions (pectin solution in our case) are typically fragile systems due to hydrogen bonding.

Doolittle's free volume theory, which contends that a molecular motion requires an empty free volume (v_f), provided another explanation for the existence of T_0 [66]. Thus, according to the Doolittle equation (Eq. 21):

$$\eta = a \cdot \exp(bv/v_f), \quad (21)$$

where v is the total volume, v_f is the fractional volume, and a , b are proportionality constants. Doolittle [66] showed that the ratio of v_f and v gives fractional volume ($f = v_f/v$) which can be related to temperature changes. As the polymer system temperature, T_K , approaches the Vogel scaling temperature, T_0 , the fractional volume f becomes zero. Thus, f decreases with a decrease in T_K , and in such circumstances, the motion of molecules decreases, and viscosity becomes high ($\eta \rightarrow \infty$ at very low temperatures and as $T_K \rightarrow T_0$) [50, 67]. However, in contrast, an increase in f (as v_f became large) led to a decrease in T_0 (i.e., $T_0 \rightarrow 0$, when system temperature increased), and as such, η will become small.

3.3. Thermodynamic parameters of BoP

Estimated values for entropy (ΔS_v) and enthalpy (ΔH_v) are presented in Table 6. The ΔS_v and ΔH_v values for results obtained using intrinsic viscosity were distributed as follows: WEp (0.056 kJ/K and 12.779 kJ/mol); AEp (0.056 kJ/K and 14.857 kJ/mol); and Cp (0.056 kJ/K and 13.386 kJ/mol), respectively. The ΔS_v and ΔH_v results obtained using apparent viscosity were as follows: dW (0.112 kJ/K and 21.991 kJ/mol); WEp (0.116 kJ/K and 23.978 kJ/mol); AEp (0.105 kJ/K and 20.660 kJ/mol); and Cp (0.104 kJ/K and 19.089 kJ/mol), respectively. In general, Table 6 shows that all values of ΔS_v were the same when considering the $[\eta]$ data. This can be expected since the values of η_0 and $(\ln \eta_0 - \Delta S_v)$ for all pectin solutions did not differ much (Table 4 and 6). The trend for ΔH_v shows that $WEp < Cp < AEp$ for intrinsic viscosity data. The apparent viscosity data showed that ΔS_v increases in order: $Cp < AEp < dW < WEp$, and for ΔH_v , $Cp < AEp < dW < WEp$ (Table 6).

The Figure 7 and Figure 8 show the linear Frenkel-Eyring plots for intrinsic viscosity and apparent viscosity, respectively. Both graphs showed a linear increase in the parameter $(\ln \eta/T_K)$ with inverse of temperature ($1/T_K$). However, as noted earlier in the Arrhenius plot, the $[\eta]$ data points were close to the line of best fit resulting in relatively high R^2 as compared to η_A data.

The ΔS_v and ΔH_v values obtained from our study for pectin samples were not far off from most of the related polysaccharides found in the literature. Malviya *et al.* [26] looked at the thermodynamic properties of tamarind seed gums and found that ΔH_v was 23.66 ± 0.97 kJ/mol and ΔS_v was -0.10 ± 0.01 kJ/K. Salehi and Kasheninejad [68] showed that ΔS_v and ΔH_v values for gums extracted

Table 6: Thermodynamic parameters of viscosity for $[\eta]$ and η_A data.

Intrinsic viscosity data						
	$(\ln \eta_0 - \Delta S_v/R)$	ΔS_v (kJ/K)	$(\Delta H_v/R)$	ΔH_v (kJ/mol)	R^2	RMSE
WEp	-15.47	0.056	1537	12.779	0.972	0.1033
AEp	-14.68	0.056	1787	14.857	0.963	0.1394
Cp	-13.87	0.056	1610	13.386	0.986	0.0776
Apparent viscosity data						
dW	-21.34	0.112	2645	21.991	0.780	0.5669
WEp	-21.11	0.116	2884	23.978	0.859	0.4716
AEp	-18.32	0.105	2485	20.660	0.904	0.3370
Cp	-17.52	0.104	2296	19.089	0.758	0.5231

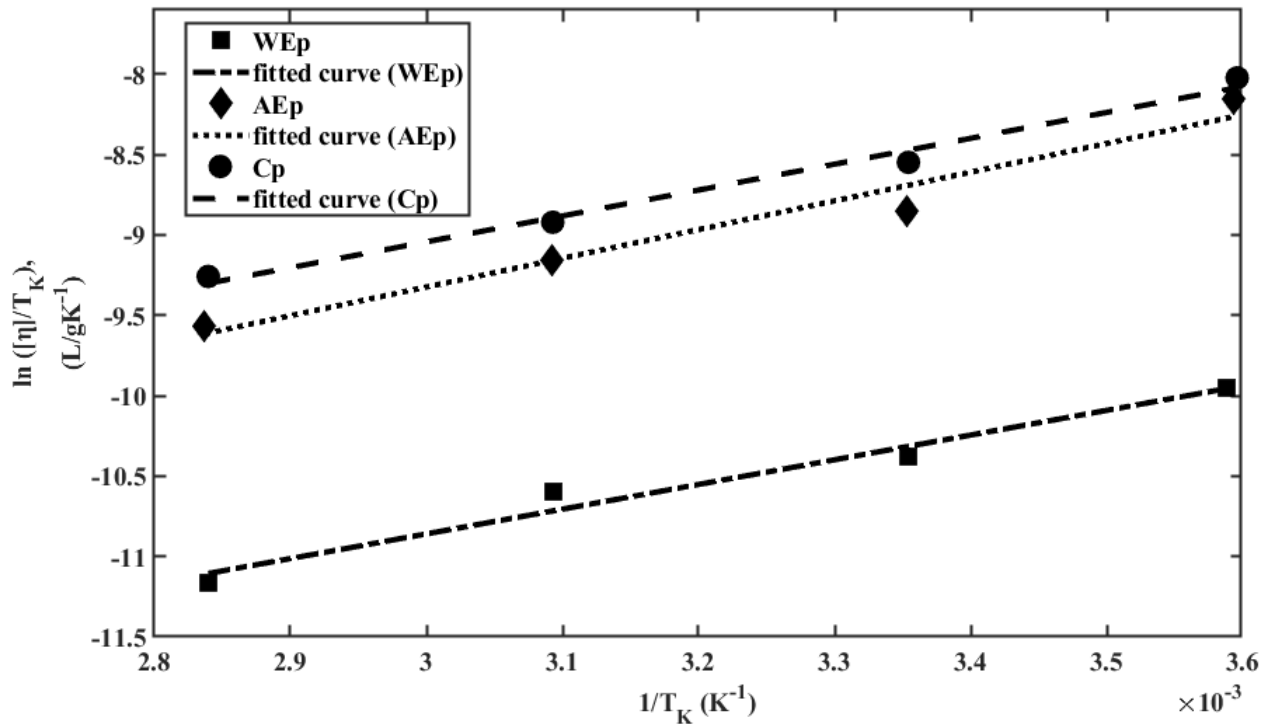


Figure 7: Frenkel-Eyring scatter plot for WEp, AEp, and Cp (intrinsic viscosity).

from wild sage seed range from 0.0063-0.0522 kJ/K and 0.52-14.99 kJ/mol, respectively. In a different study, Eddy *et al.* [69] used Eucalyptus Citriodora gums and found that the entropy ΔS_v was -55.77 kJ/K and the enthalpy (ΔH_v) was 14.09 kJ/mol.

It is known that the polarity (negativity or positivity) of the entropy and enthalpy is of great importance in deducing viscous flow [49, 69, 70]. Eddy *et al.* [69] showed that negative entropy (ΔS_v^-) and positive enthalpy (ΔH_v^+) found in Eucalyptus Citriodora gums' temperature dependence suggest that viscous flow is attained by bond breaking. According to Ahmad *et al.* [71] and Eddy *et al.* [72], ΔS_v^- is linked to the uncoiling orientation of polymer molecules. This is why the polymer system is more organised in viscous flow. Acevedo and Katz [49] further showed that at ΔS_v^- (negentropy), polymer molecules become less disorderly or more ordered. Salehi *et al.* [70] said that negentropy, ΔS_v^- , suggests the creation of an activated complex for phase changes or viscous flow. This leads to more ordered molecules, which makes the flow viscous. ΔS_v^+ shows that when an activated complex forms, the more ordered hydrogen bond has to be stretched or broken, which leads to less molecular order [49, 70]. However, Kauzman [73] says that other bonds, like electrostatic and hydrophobic interactions, get stronger with increase in ΔS_v . Ahmad *et al.* [70] stated that ΔH_v^+ is the energy needed by gum molecules to jump from one position to another, which is similar to potential energy barrier, E_a . Salehi *et al.* [70] and Amin *et al.* [74] explained that ΔS_v^+ indicates that the process is reversible.

Table 6 shows that both entropy and enthalpy were both positive, ΔS_v^+ and ΔH_v^+ . This means that the polymeric systems become disordered and need energy to break bonds in order to reach a transition state and allow fluid flow. Therefore, it can be generalised that WEp and dW were more disordered (higher values of ΔS_v^+) and required relatively less energy for bond breaking (lower values

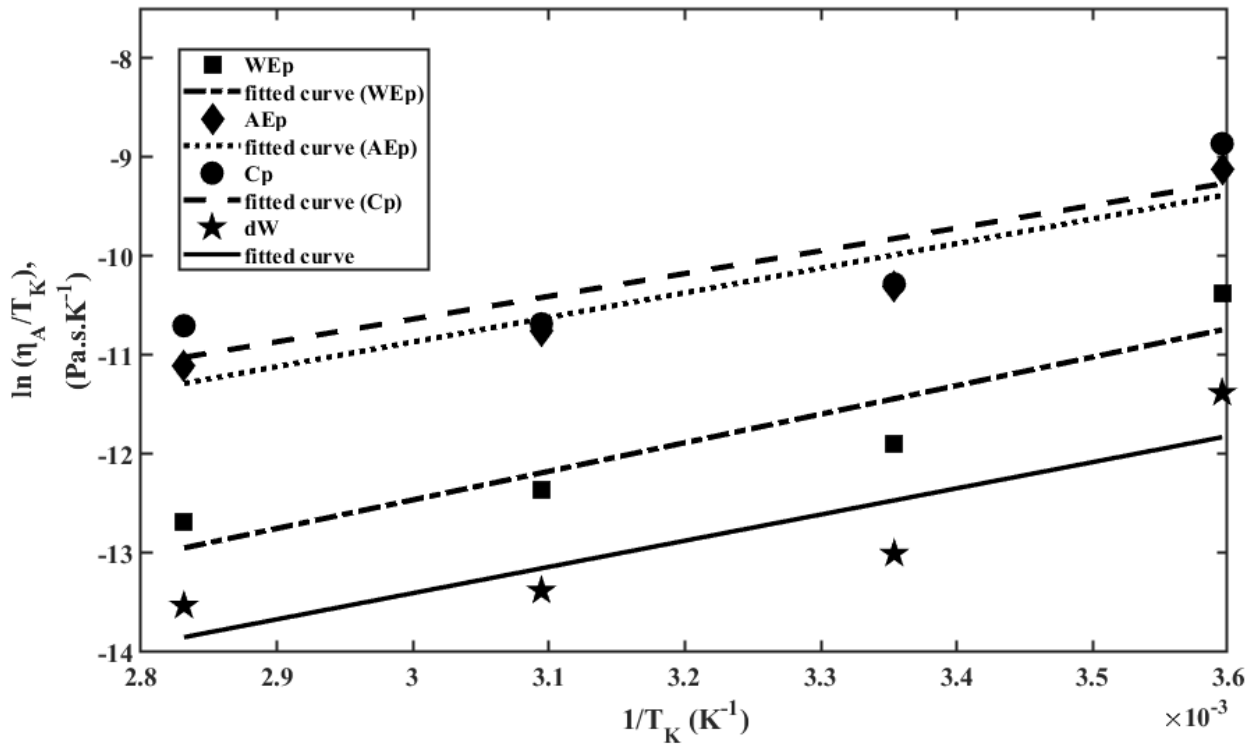


Figure 8: Frenkel-Eyring scatter plot for WEp, AEp, and Cp (apparent viscosity).

of ΔH_v^+) as compared to AEp and Cp. This was seen because molecules had different molecular weights, degrees of esterification, and sizes [72], which led to different viscosity properties (see Table 1 and 2).

The Gibbs-Helmholtz equation (Eq. 18) uses entropy ΔS_v and enthalpy ΔH_v to find the free energy, or Gibbs energy, ΔG_v . This means that the values of ΔH_v and ΔS_v determine the sign and size of ΔG_v . The values for Gibbs free energy are shown in Table 7. The (ΔG_v^-) for $[\eta]$ and η_A were calculated using pre-exponential from Table 3 and Table 4, respectively. All values were observed to be negative (ΔG_v^-), and the magnitude of Gibbs energy became low with an increase in temperature (Table 7). Considering the temperature range of 278.16-353.16 K, values of ΔG_v were distributed as follows: WEp (-2.681 to -6.984 kJ); AEp (-0.751 to -4.914 kJ); and Cp (-2.209 to -6.363 kJ) for intrinsic viscosity data. ΔG_v values for data calculated from apparent viscosity were as follows: WEp (-8.227 to -16.911 kJ); AEp (-8.574 to -16.457 kJ); Cp (-9.792 to -17.580 kJ); and dW (-9.191 to -17.598 kJ). In general, the values increase in the order: $WEp < Cp < AEp$ for $[\eta]$ data and $dW < WEp < Cp < AEp$ for η_A data at approximately the same temperature.

Malviya *et al.* [26] found ΔG_v values of -55.46 ± 1.69 kJ for temperature-dependent viscosity tamarind seed gums. They said that the value was pretty low, which shows that there are not many interactions between or within molecules. The results from this study may suggest that there were more interactions since the values of ΔG_v were higher compared to Malviya *et al.* [26]. Thus, the lower the ΔG_v (as the value becomes more negative), the more ‘spontaneous’ the pectin solution moves towards viscous flow. For example, looking at intrinsic viscosity data, a ΔG_v value of -2.681 kJ/mol was found for the WEp sample at 278.16 K. This suggests that at the same temperature, WEp solution was easier to flow (low $[\eta]$; Table 1) than AEp (high viscosity; $\Delta G_v = -0.751$ kJ/mol) (Table 7). The value of ΔG_v becomes more negative as temperature increases for all pectin solutions; this can be a feature of temperature-dependent flow, where solutions can easily flow at higher temperatures as compared to low temperatures. Rao [22], and Adam and Gibbs [30] explain this as associated with changes in the molecular interactions (breaking, stretching, and shifting of chemical bonds). Another significant trend was observed in the $[\eta]$ data: ΔG_v increased as the value of enthalpy ΔH_v increases. For example, AEp has both high ΔH_v and ΔG_v followed by Cp and lastly WEp. However, this is only valid when entropy ΔS_v is fairly constant for all pectin solutions as observed in Table 6. This was not the case in the η_A data. The polarity of ΔS_v and ΔH_v , which was earlier noted, can also support spontaneity (readiness to flow). Winzor and Jackson [75] specified that if both ΔS_v and ΔH_v are positive for a particular thermodynamic system, ΔG_v will always be negative over a certain temperature range, hence its susceptibility to flow spontaneously. The reason might be due to the term $T_K \cdot \Delta S_v$, which is always subtracted from ΔH_v (Eq. 18); thus, as temperature T_K increases, $T_K \cdot \Delta S_v$ also becomes large while ΔH_v remains fairly constant, and hence, at a certain temperature range, $T_K \cdot \Delta S_v > \Delta H_v = -\Delta G_v$.

Table 7: Gibbs free energy values of $[\eta]$ and η_A at specific temperatures.

Pectin	Intrinsic viscosity, $[\eta]$ data		Apparent viscosity, η_A data	
	T_K , (K)	$-\Delta G_v$ (kJ)	T_K (K)	$-\Delta G_v$ (kJ)
WEp	278.69	2.681	278.16	8.227
	298.12	3.952	298.16	10.543
	323.26	5.362	323.16	13.438
	352.16	6.984	353.16	16.911
AEp	278.26	0.751	278.16	8.574
	298.26	1.872	298.16	10.677
	323.43	3.284	323.16	13.304
	352.49	4.914	353.16	16.457
Cp	278.09	2.209	278.16	9.792
	298.13	3.333	298.16	11.869
	323.33	4.746	323.16	14.465
	352.16	6.363	353.16	17.580
dW			278.16	9.191
			298.16	11.433
			323.16	14.235
			353.16	17.598

4. Conclusion

The viscosity-temperature dependence of BoP (WEp and AEp) at 278.16-353.16 K showed that the viscosity of the pectin solution decreases as the temperature increases. The activation energy (E_a), rate at which the flow of BoP solution changes, depends on the initial viscosity of the solution. The higher the viscosity (AEp and Cp solution), the higher the temperature (activation energy) needed, and the lower the viscosity (WEp), the lower the temperature needed to initiate flow. Based on the pre-exponential factor (η_0), it was concluded that in WEp (lower values of η_0), only a small number of molecules were needed for temperature-independent motion to start. On the other hand, in AEp and Cp, where η_0 was higher, a greater number of molecules were required. The apparent viscosity data showed a non-linear relationship with temperature, since the best fit model was a non-linear Vogel-Fulcher-Tammann-Hesse (VFTH) model rather than the common linear Arrhenius model. This difference between η_A and $[\eta]$ was attributed to the sensitiveness of the testing methods and the wider temperature range used. The study also emphasised the significance of Arrhenius activation temperature, or Boltzmann factor (T^*), Arrhenius temperature (T_A), and Vogel scaling temperature, or vitreous transition temperature (T_O), as temperature constants associated with specific flow transitions. The Frenkel-Eyring equation gave the thermodynamic parameters that showed all pectins become disordered when temperature is raised (positive entropy, ΔS_v), and they also need heat energy to break or stretch bonds when they reach the transition state (positive enthalpy, ΔH_v). The Gibbs free energy (ΔH_v) was negative for all pectins, indicating that when the temperature was increased, the flow of pectin solution become spontaneous. Based on the thermodynamic parameters, WEp solutions were more likely to flow (less viscous) as compared to AEp at any given temperature. The analysis of temperature dependence on the flow of BoP solution, illustrated in this study, can be of importance in product development and process design. However, more research needs to be done on how temperature affects the shape factors, molecularity, hydrodynamic radius, and voluminosity of baobab pectin.

Acknowledgment

The Food Processing Technology Department and the Mathematical Sciences Department at Harare Institute of Technology (H.I.T.) supported this study. Special thanks to the Food Analysis Laboratory at H.I.T. for helping in set up our experiments. We appreciate Professor M. A. N. Benhura (University of Zimbabwe) for his advisory input during the progression of this study. There are no special grants or other forms of funding received for this research, and no areas of conflict have been recorded to the best knowledge of the authors.

References

- [1] B. K. Ndabikunze, B. N. Masambu, B. P. M. Tiisekwa & A. Issa-Zacharia, "The production of jam from indigenous fruits using baobab (*Adansonia Digitata* L.) powder as a substitute for commercial pectin", African Journal of Food Science 5 (2011) 168. <https://academicjournals.org/journal/AJFS/article-stat/51E20113089>
- [2] O. A. Patova, A. Luanda, N. M. Paderin, S. V. Popov, J. J. Makangara, S. P. Kuznetsov & E. N. Kalmykova, "Xylogalacturonan enriched pectin from the fruit pulp of *Adansonia digitata* Structural characterization and antidepressant like effect", Carbohydrates Polymer 262 (2021) 11746. <https://doi.org/10.1016/j.carbpol.2021.117946>

- [3] K. Alba, V. Offiah, A. P. Laws, K. O. Falade & V. Kontogiorgos, "Baobab polysaccharides from fruits and leaves", *Food Hydrocolloids* **106** (2020) 105874. <https://doi.org/10.1016/j.foodhyd.2020.105874>
- [4] S. Damodaran, K. L. Parkin & O. R. Fennema, *Fennema's Food Chemistry*, CRC press: Taylor and Francis Group LLC, Boca Raton, United States of America, 2008, pp. 146-147. https://www.academia.edu/8361211/Fennemas_Food_Chemistry_4th_edition_pdf
- [5] A. A. Sundar Raj, S. Rubila, R. Jayabalan & T. V. Ranganathan, "A review on Pectin: Chemistry due to general properties of Pectin and its pharmaceutical uses", *Scientific Reports* **1** (2012) 2. https://www.researchgate.net/publication/281388262_A_review_on_pectin_Chemistry_due_to_general_properties_of_pectin_and_its_pharmaceutical_uses
- [6] A. A. Nour, B. I. Magboul & N. H. Kheiri, "Chemical composition of baobab fruit (*Adansonia Digitata* L.)", *Food Research Centre, Khartoum North* (1980) 1. https://www.doc-developpement-durable.org/file/Culture/Arbres-Fruitiere/FICHES_ARBRES/baobab/Chemical%20composition%20of%20baobab%20fruit%20Adansonia%20digitata.pdf
- [7] M. Dimopoulou, K. Alba, I. A. Sims & V. Kontogiorgos, "Structure and rheology of pectic polysaccharides from baobab fruit and leaves", *Carbohydrate Polymers* **273** (2021) 118540. <https://doi.org/10.1016/j.carbpol.2021.118540>
- [8] L. M. Nwokocha & P. A. Williams, "Rheological properties of a polysaccharide isolated from *Adansonia digitata* leaves", *Food Hydrocolloids* **58** (2016) 29. <https://doi.org/10.1016/j.foodhyd.2016.02.013>
- [9] I. C. M. Dea & A. Morrison, "Chemistry and interactions of seed galactomannans", *Advances in Carbohydrate Chemistry and Biochemistry* **32** (1975) 241. [https://doi.org/10.1016/S0065-2318\(08\)60298-X](https://doi.org/10.1016/S0065-2318(08)60298-X)
- [10] M. A. Masuelli, "Viscometric study of pectin. Effect of temperature on the hydrodynamic properties", *International Journal of Biological Macromolecules* **48** (2011) 286. <https://doi.org/10.1016/j.ijbiomac.2010.11.014>
- [11] T. Tanglerpaibul & M. A. Rao, "Intrinsic viscosity of tomato serum as affected by methods of determination and methods of processing concentrates", *Journal of Food Science* **52** (1987) 1642. <https://doi.org/10.1111/j.1365-2621.1987.tb05895.x>
- [12] R. Pamies, J. G. Hernández Cifre, M. del Carmen Lopez Martínez, & J. de la Torre, "Determination of intrinsic viscosities of macromolecules and nanoparticles. Comparison of single-point and dilution procedures", *Colloid and Polymer Science* **286** (2008) 1223. <https://doi.org/10.1007/s00396-008-1902-2>
- [13] F. Behrouzian, S. M. A. Razavi & H. Karazhiyan, "Intrinsic viscosity of cress (*Lepidium sativum*) seed gum: Effect of salts and sugars", *Food Hydrocolloids* **35** (2014) 100. <https://doi.org/10.1016/j.foodhyd.2013.04.019>
- [14] G. A. van Aken, *Polysaccharides in food emulsions. Food polysaccharides and their applications*, Taylor & Francis Group, Boca Raton, United States of America, 2006, pp. 521. https://www.researchgate.net/publication/279724123_Polysaccharides_in_Food_Emulsions
- [15] S. Muyambo, I. Chikurunhe, & D. N. Moyo, "Intrinsic viscosity of *Stud* Plant Mucilage (*Dicerocaryum Zanguebarium*): Polymeric Studies at Infinite Dilution", *Journal of Modern Chemistry & Chemical Technology* **10** (2019) 28. <https://sciencejournals.stmjournals.in/index.php/RRJoFST/article/view/3090>
- [16] S. M. A. Razavi, T. M. Moghaddam, B. Emadzadeh & F. Salehi, "Dilute solution properties of wild sage (*Salvia macrosiphon*) seed gum", *Food Hydrocolloids* **29** (2012) 205. <https://doi.org/10.1016/j.foodhyd.2012.02.020>
- [17] M. Tahir, R. E. Hincapie, M. Be & L. Ganzer, "A comprehensive combination of apparent and shear viscoelastic data during polymer flooding for EOR evaluations", *World Journal of Engineering and Technology* **5** (2017) 585. <https://doi.org/10.4236/wjet.2017.54050>
- [18] P. J. Fellows, *Food processing technology: Principle and practice*, CRC Press, New York, United States of America, 2009, pp. 13-17 <https://shop.elsevier.com/books/food-processing-technology/fellows/978-1-84569-216-2>
- [19] C. G. Lopez, R. H. Colby & J. I. B. Cabral, "Electrostatic and hydrophobic interactions in NaCMC aqueous solutions: Effect of degree of substitution", *Macromolecules* **51** (2018) 3165. <https://doi.org/10.1021/acs.macromol.8b00178>
- [20] M. Berthelot, "Essaie dune theorie sur la formation des ethers", *Annals de chimie et de physique*. **T66** (1862) 110. <https://www.loc.gov/item/49052172/>
- [21] J. Belehradek, "Sur la signification des coefficients de temperature", *Protoplasma* **7** (1929) 232. <https://doi.org/10.1007/BF01612807>
- [22] M. Rao, "Flow and functional models for rheological properties of fluid foods", in *Rheology of Fluid, Semisolid, and Solid Foods. Food Engineering Series*, Springer, Boston MA, United States of America, 2013, pp. 27-61. https://doi.org/10.1007/978-1-4614-9230-6_2
- [23] J. H. Van't Hoff, *Studies in chemical dynamics*, F. Muller & Co, Amsterdam, Netherlands, 1896, pp. 122-126. <https://archive.org/details/studiesinchemica00hoffrich>
- [24] S. Vyazovkin, "Activation energies and temperature dependencies of the rate of crystallization and melting of polymers", *Polymers* (2020) 1. <https://doi.org/10.3390/polym12051070>
- [25] A. Messaadi, N. Dhoubi, H. Hamda, F. B. M. Belgacem, Y. H. Abdelkader, N. Ouerfelli & A. H. Hamzaoui, "A new equation relating the viscosity Arrhenius temperature and the activation energy for some Newtonian classical solvents", *Journal of Chemistry* (2015) 1. <https://doi.org/10.1155/2015/163262>
- [26] R. Malviya, S. Jha, N. K. Fuloria, V. Subramaniyan, S. Chakravarthi, K. Sathasivam, U. Kumari, D. U. Porwai, A. Sharma & D. H. Kumar, "Determination of temperature-dependent coefficients of viscosity and surface of Tamarind seeds (*Tamatindus indica* L.) polymer", *Polymer* **13** (2021) 1. <https://doi.org/10.3390/polym13040610>
- [27] R. B. Haj-Kacem, N. Ouerfelli, J. V. Herráez, M. Guettari, H. Hamda & M. Dallel, "Contribution to modeling the viscosity Arrhenius-type equation for some solvents by statistical correlations analysis", *Fluid Phase Equilibria* **383** (2014) 11. <https://doi.org/10.1016/j.fluid.2014.09.023>
- [28] P. Atkins & J. de Paula, *Physical chemistry*, W. H. Freeman, New York, United States of America, 2014, pp. 212-234. https://www.academia.edu/93378803/Peter_Atkins_Julio_de_Paula_Physical_Chemistry_Thermodynamics_Structure_and_Change_Freeman_and_Co_2014_
- [29] E. Ike, "Arrhenius-type relationship of viscosity as a function of temperature for mustard and cotton seed oils", *International Research Journal of Pure and Applied Physics* **9** (2021) 44. <https://ejournals.org/irjpp/vol-8-issue-2-2021/arrhenius-type-relationship-of-viscosity-as-a-function-of-temperature-for-mustard-and-cotton-seed-oils/>
- [30] G. Adam & J. H. H. Gibbs, "On the temperature dependence of cooperative relaxation properties in glass-forming liquids", *Journal of Chemistry and Physics* **43** (1965) 139. <https://doi.org/10.1063/1.1696442>
- [31] M. Aniya, & T. Shinkawa, "A model for the fragility of metallic glass forming liquids", *Material Transactions* **48** (2007) 1793. <https://doi.org/10.2320/matertrans.MJ200737>
- [32] M. Ikeda & M. Aniya, "Bond Strength-Coordination Number Fluctuation Model of Viscosity: An Alternative Model for the Vogel-Fulcher-Tammann Equation and an Application to Bulk Metallic Glass Forming Liquids", *Materials* **3** (2010) 5246-5262. <https://doi.org/10.3390/ma3125246>
- [33] M. P. Cox & E. H. H. Merz, "Correlation of dynamic and steady flow viscosities", *Journal of Polymer Science* **28** (1958) 616. <http://dx.doi.org/10.1002/pol.1958.1202811812>
- [34] I. T. S. Li, *Hydrophobic hydration of a single polymer*, Ph.D. thesis, Department of Chemistry, University of Toronto, Toronto, Canada, 2012. <https://tspace.library.utoronto.ca/handle/1807/34783>
- [35] R. L. Baldwin, "Temperature-dependence of the hydrophobic interaction in protein folding", *Proceedings of the National Academy of Science* **83** (1986) 8069. <https://doi.org/10.1073/pnas.83.21.8069>
- [36] M. A. Masuelli, "Mark-Houwink parameters for aqueous soluble polymers and biopolymers at various temperatures", *Journal of Polymer and Biopolymer Physics Chemistry* **2** (2014) 37. <http://www.sciepub.com/reference/256766>
- [37] F. Kar & N. Arslan, "Effect of temperature and concentration on viscosity of orange peel pectin solutions and intrinsic viscosity-molecular weight relationship", *Carbohydrate Polymers* **40** (1999) 277. [https://doi.org/10.1016/S0144-8617\(99\)00062-4](https://doi.org/10.1016/S0144-8617(99)00062-4)

- [38] Z. Zamani & S. M. A. Razavi, "Molecular parameters and intrinsic viscosity of Nettle Seed (*Urtica Pilulifera*) gum as a function of temperature", Pre-prints Research Square. <https://doi.org/10.21203/rs.3.rs-151482/v1>
- [39] K. Monkos, "On the hydrodynamics and temperature dependence of the solution conformation of human serum albumin from viscometry approach", *Biochimica et Biophysica Acta* **1700** (2004) 27. <https://doi.org/10.1016/j.bbapap.2004.03.006>
- [40] Z. K. Muhidinov, Kh Kh. Avloev, M. T. Norova, A. S. Nasriddinov & D. Kh Khalikov, "Effect of temperature on the intrinsic viscosity and conformation of different pectins", *Polymer Science Series A* **52** (2010) 1257. <https://doi.org/10.1134/S0965545X10120035>
- [41] M. Y. Sayah, R. Chabir, H. Benyahia, Y. Rodi Kandri, F. Ouazzani Chahdi, H. Touzani & F. Errachidi, "Yield, esterification degree and molecular weight evaluation of Pectins isolated from orange and grapefruit peels under different conditions", *PLoS ONE* **11** (2016) 1. <https://doi.org/10.1371/journal.pone.0161751>
- [42] A. Walding, "Pectin rich fruit", Livestrong, Com, 2011. [Online]. <https://www.livestrong.com/>
- [43] S. Muyambo, "Analysis of the intrinsic viscosity behaviour in polymer mixtures of Stud Plant Mucilage (*Dicerocaryum zanguebarium*) with Carboxymethyl cellulose and Guar gum: Synergism at infinite dilution", *Research & Reviews: Journal of Food Science & Technology* **10** (2021) 1. <https://sciencejournals.stmjournals.in/index.php/RRJoFST/article/view/3090>
- [44] M. A. Masuelli, "Intrinsic viscosity determination of high molecular weight biopolymers by different plot methods. Chia Gum Case", *Journal of Polymer and Biopolymer Physics and Chemistry* **6** (2018) 13. <https://doi.org/10.12691/jpbpc-6-1-2>
- [45] A-A. A. Abel-Azim, A. M. Atta, M. S. Farahat & W. Y. Boutros, "Determination of intrinsic viscosity of polymeric compounds through a single specific viscosity measurement", *Polymers* **39** (1998) 6827–6833. [https://doi.org/10.1016/S0032-3861\(98\)00184-0](https://doi.org/10.1016/S0032-3861(98)00184-0)
- [46] A. K. Mahanta & P. K. S. Pattnayak, "Green analytical methods for the determination of intrinsic viscosity of hydroxyl terminated polybutadiene", *Journal of Material and Environmental Science* **6** (2015) 2377. <https://api.semanticscholar.org/CorpusID:19661982>
- [47] N. Ouerfelli, M. Bouaziz & J. V. Herrera, "Treatment of Herrera equation correlating viscosity in binary liquid mixtures exhibiting strictly monotonous distribution", *Physics and Chemistry of Liquids* **51** (2013) 55. <https://doi.org/10.1080/00319104.2012.682260>
- [48] G. Tammann & W. Hesse, "Die Abhängigkeit der Viscosität von der Temperatur bei unterkühlten Flüssigkeiten", *Zeitschrift für Anorganische und Allgemeine Chemie* **156** (1926) 245. <https://doi.org/10.1002/zaac.19261560121>
- [49] I. L. Acevedo, & M. P. Kartz, "Viscosities and thermodynamics of various flows of some binary mixtures at different temperatures", *Solution Chemistry* **19** (1990) 1041. <https://doi.org/10.1007/BF00650507>
- [50] M. Sillick & C. M. Gregson, "Viscous fragility of concentrated maltopolymer/ sucrose mixtures", *Carbohydrate Polymers* **78** (2009) 879. <https://doi.org/10.1016/j.carbpol.2009.07.015>
- [51] E. Ike & S. C. Ezike, "Estimation of viscosity Arrhenius pre-exponential factor and activation energy of some organic liquids". *International Journal of Recent Research in Physics and Chemical Science* **5** (2018) 18. <http://docplayer.net/212753187-Estimation-of-viscosity-arrhenius-pre-exponential-factor-and-activation-energy-of-some-organic-liquids.html>
- [52] V. Jagannadham, "How do we introduce the Arrhenius pre-exponential factor (A) to graduate students?", *Creative Education* **2** (2010) 128. <http://dx.doi.org/10.4236/ce.2010.12019>
- [53] H. Eyring & J. E. Hirschfelder, "The theory of the liquid state", *Journal of Physical Chemistry* **41** (1937) 249. <https://doi.org/10.1021/j150380a007>
- [54] R. C. M. de Paula, S.A. Santana & J. F. Rodrigues, "Composition and rheological properties of Albizia lebeck gum exudate", *Carbohydrate Polymers* **44** (2001) 133. [https://doi.org/10.1016/S0144-8617\(00\)00213-7](https://doi.org/10.1016/S0144-8617(00)00213-7)
- [55] R. de Paula & J. F. E. Rodrigues, "Composition and rheological properties of cashew tree gum, the exudate polysaccharide from *Anacardium occidentale* L.", *Carbohydrate Polymers* **26** (1995) 177. [https://doi.org/10.1016/0144-8617\(95\)00006-S](https://doi.org/10.1016/0144-8617(95)00006-S)
- [56] G. T. Mezger, *The rheology handbook: For users of rotational and oscillatory rheometers*, Elsevier, New York, United States of America, 2006, pp. 19-78. <https://shorturl.at/zKRU6>
- [57] Z. Berk, *Food process engineering and technology*, Elsevier Inc, New York, United States of America, 2009, pp. 115-124. <https://www.sciencedirect.com/book/9780123736604/food-process-engineering-and-technology>
- [58] M. Shaikh, M. Shafique, B. R. Aggarwal & M. Farooqui, "Density, viscosity, and activation parameters of viscous flow for cetrimide in ethanol + water system at 301.5 K", *Rasayan Journal of Chemistry* **4** (2011) 172. https://www.researchgate.net/publication/279558087_Density_viscosity_and_activation_parameters_of_viscous_flow_for_cetrimide_in_ethanol_water_system_at_3015_K
- [59] C-W. Liew & S. Ramesh, "Electrical, structural, thermal, and electrochemical properties of corn starch-based biopolymer electrolytes", *Carbohydrate Polymers* **124** (2015) 222. <https://doi.org/10.1016/j.carbpol.2015.02.024>
- [60] T. Sogabe, A. E. Granados, S. Fong-IN & K. Kawai, "Effect of glass transition temperature on the viscosity of carbohydrate solutions and fruit juices as functions of temperature and solute concentration", *Cryobiology and Cryotechnology* **67** (2021) 103. <https://doi.org/10.20585/cryobolcryotechnol.67.2.103>
- [61] C. A. Angell, R. D. Bressel, J. L. Green, H. Kanno, M. Oguni & E. J. Sare, "Liquid fragility and the glass transition in water and aqueous solutions", *Journal of Food Engineering* **22** (1994) 115. [https://doi.org/10.1016/0260-8774\(94\)90028-0](https://doi.org/10.1016/0260-8774(94)90028-0)
- [62] F. Frank, *Water: A matrix of life*, Royal Society of Chemistry, Cambridge, United Kingdom, 2000, pp. 15-29. <https://www.perlego.com/book/786943/water-a-matrix-of-life-pdf>
- [63] Y. H. Roos & M. Karel, "Water and molecular weight effects on glass transitions in amorphous carbohydrates and carbohydrate solutions", *Journal of Food Science* **56** (1991) 1676. <https://doi.org/10.1111/j.1365-2621.1991.tb08669.x>
- [64] C. A. Angell, K. L. Ngai, G. B. McKenna, P. F. McMillan & S. W. Martin, "Relaxation in glass forming liquids and amorphous solids", *Journal of Applied Physics* **88** (2000) 3113. <https://doi.org/10.1063/1.1286035>
- [65] J. F. Mano & E. Pereira, "Data analysis with the Vogel-Fulcher-Tammann-Hesse equation", *Journal of Physical Chemistry A* **108** (2004) 10824. <https://doi.org/10.1021/jp0484433>
- [66] A. K. Doolittle, "Studies in Newtonian flow. I. The dependence of the viscosity of liquids on temperature", *Journal of Applied Physics* **22** (1951) 1031. <https://doi.org/10.1063/1.1700096>
- [67] M. H. Cohen & G. S. Grest, "Liquid-glass transition, a free-volume approach", *Physical Review B* **20** (1979) 1077. <https://doi.org/10.1103/PhysRevB.20.1780>
- [68] F. Salehi & M. Kashaninejad, "Kinetics and thermodynamics of gum extraction from wild sage seed", *International Journal of Food Engineering* **10** (2014) 625. <https://doi.org/10.1515/ijfe-2014-0079>
- [69] N. O. Eddy, I. Udofia, A. Uzairu, A. O. Odiongenyi, C. Obadimu "Physicochemical, spectroscopic and rheological studies on *Eucalyptus Citriodora* (EC) gum", *Journal of Polymer and Biopolymer Physics Chemistry* **52**(2015) 5220. <http://www.sciepub.com/abstract/abstract.aspx?id=jpbpc&num=1554>
- [70] F. Salehi, M. Kashaninejad, A. Tadayyon & F. Arabameri, "Modeling of extraction process of crude polysaccharides from Basil seeds (*Ocimum basilicum* L.) as affected by process variables", *Journal of Food Science and Technology* **52** (2015) 5220. <https://doi.org/10.1007/s13197-014-1614-1>
- [71] N. Ahmad, A. Saeed, K. Ahad & M. S. Khan, "Effect of temperature of dilute polyelectrolyte solutions", *Journal of Chemical Society of Pakistan* **16** (1994) 91. <https://jcspp.org.pk/issueDetail.aspx?aid=628e148a-29e6-44f7-8138-effe984c8b8e>
- [72] N. O. Eddy, P. O. Ameh, C. E. Gimba & E. E. Ebenso, "Rheological modelling and characterization of *Ficus platyphylla* gum exudates", *Journal of Chemistry* (2013) 1. <https://doi.org/10.1155/2013/254347>
- [73] W. Kauzman, "Some factors in the interpretation of protein denaturation", *Advance in Protein Chemistry* (1959) 51. [https://doi.org/10.1016/s0065-3233\(08](https://doi.org/10.1016/s0065-3233(08)

60608-7

- [74] S. Amin, G. Hawash, E. Diwani & El Rafei, "Kinetics and thermodynamics of oil extraction from jatropha curcas in aqueous acidic hexane solutions", Journal of American Science **6** (2010) 1. <https://scirp.org/reference/referencespapers.aspx?referenceid=1558944>
- [75] D. J. Winzor & C. M. Jackson, "Interpretation of the temperature dependence of equilibrium and rate constants", Journal of Molecular Recognition **19** (2006) 389. <https://doi.org/10.1002/jmr.799>

APPENDIX A.

Experimental data Link

Gelation, hydrodynamic and temperature-dependency properties of baobab pectin. Mendeley Data, V1. <https://doi.org/10.17632/j4p4dnr5rh.1>